Phonon-assisted indirect recombination of bound excitons in N-doped GaP, including near-resonant processes

Honghai Dai and Martin A. Gundersen
Department of Electrical Engineering and Department of Physics, University of Southern California, Los Angeles, California 90089-0484

Charles W. Myles
Department of Physics and Engineering Physics, Texas Tech University, Lubbock, Texas 79409-4180

Paul G. Snyder
Department of Electrical Engineering, University of Nebraska–Lincoln, Lincoln, Nebraska 68588-0511
(Received 29 December 1986; revised manuscript received 23 July 1987)

The phonon sideband spectrum of bound excitons in N-doped GaP is calculated using a model wherein intrinsic lattice phonons assist momentum conservation through indirect electron-hole recombination at the impurity site. Detailed comparisons are made of the spectrum obtained on the basis of this model and the experimental spectrum. These comparisons are used to demonstrate that near-resonant processes strongly affect the phonon-assisted indirect recombination and thus that such processes are important in the determination of the shape of the phonon sideband spectrum. Using this phonon sideband theory, two models for the N-impurity wave function are tested by comparing the sideband spectra calculated using these models with the experimental spectrum. Finally, by including a configuration-coordinate-type coupling for the optic phonons, it is demonstrated that some of the low-energy structure observed in the luminescence spectrum can be interpreted as replicas of the spectrum described by the indirect transition model.

I. INTRODUCTION

The luminescence spectrum of nitrogen-bound excitons in GaP includes well-resolved phonon sidebands due to recombination assisted by phonons with energies which correspond to the lattice vibrations at various points in the Brillouin zone, and the intensity of these sidebands is very strong at low temperatures.[1,2] Various models have been proposed to explain these sidebands, including a direct-transition model[2,3] and a configuration coordinate (CC) model[3] of the electron-phonon coupling. In previous papers, it was shown that many features of this phonon sideband spectrum can be qualitatively explained by an indirect transition model.[4–6] In the present paper the physics of the processes which produce this spectrum is further explored within the context of the latter model, and the near-resonant processes which contribute to the phonon-assisted recombination in this system are studied. In particular, it is shown in this paper that near-resonant, indirect processes can play a significant role in determining the shape and the positions of the peaks in the phonon sideband structure of N-bound excitons in GaP, and that such processes may also provide clues to the reasons for the high quantum efficiency of radiative recombination in this system. In addition, it is shown that some properties of the defect-host system, such as the defect-state wave function, the phonon densities of states and dispersion relations, and electron-phonon scattering matrix elements, can be studied from the calculation of the phonon sidebands.[4–6]

Both direct and indirect transitions can occur in indirect band-gap semiconductors through bound states, in some cases. For example, in the luminescence spectra of GaP:S, GaP:Se, GaP:Te,[7] the no-phonon lines are considered to originate with the direct decay of the bound exciton, and the bound exciton phonon sidebands are attributed to an indirect decay process in which momentum-conserving phonons are involved.

The difference between GaP:N and either GaP:Se, GaP:Te, or GaP:S is that GaP:N results in a "deep" (deep in the sense that the electron wave function is highly localized even though electron binding energy is only ~ 10 meV) trap state for the bound electron while GaP:Se, GaP:Te, and GaP:S result in shallow trap states. The CC coupling model is widely accepted for studying transitions related to deep-trap states, because a deep-trap state normally causes a bigger Franck-Condon shift than a shallow trap state does. However, if the Franck-Condon shifts are small for some deep-trap states, it can be appropriate to use the indirect transition model to study the transitions related to phonon sidebands.

The Huang-Rhys factor of GaP:N is less than 0.5.[8] This suggests using the indirect transition model to study the phonon sideband spectrum of GaP:N. Furthermore, as is shown below, in comparison with the CC model, the indirect transition model is needed to study certain phonon sidebands of GaP:N in detail.

Specific evidence for the need for the indirect transition model for the GaP:N phonon sidebands includes the following.

(1) The state density spectrum of the transverse acoustic (TA) phonons of GaP shows a peak at ~ 11 meV. If the impurity wave function of GaP:N was a constant over all the Brillouin zone, the peak of the A-TA phonon sideband would then be located at ~ 11 meV below the no-phonon A line based on the indirect transition model. However, the deep-trap state wave function of GaP:N shows that the wave function is mainly located at the X point of the Brillouin zone and the TA phonon energy at the X point is ~ 13 meV. If the density of states of the TA phonons were a constant, the peak of the A-TA phonon sideband would be located at ~ 13 meV below the no-phonon line based on the indirect transition model also. Because of the combination of the TA phonon state density and the distribution of the impurity wave functions, the peak of the A-TA sideband is located at ~ 12 meV below the no-phonon A line. Furthermore, the phonons with energy ~ 12 meV correspond to K-vector-dependent states with lower symmetry than those belonging to the X and L points of the Brillouin zone. There is a large energy splitting effect at the lower symmetry points of the two branches of the transverse acoustic phonons. This is why there are two peaks in the A-TA-phonon sideband. We are not able to explain these features using a CC model because the K vector dependent effects of both the impurity wave function and phonon energy are not included in such a model.

(2) In the GaP:N luminescence spectrum there are two LO (longitudinal optical) phonon sidebands. One comes from the transition in which electron couples with the LO phonon at the Γ point of the Brillouin zone, the other one comes from the transition in which electron couples with the phonon at the X point. The CC model is appropriate for calculating the A-LO(Γ) band, because of the strong coupling between the electron and the phonon at the Γ point, which is an example of the Frohlich interaction. However, when couplings between the electron and phonons at points other than the Γ point are considered, the CC model does not favor specific points in the Brillouin zone. In other words, except at the zone center, there is not a big difference between the phonons at the X point and at the L point or at some other points based on the CC model, since K-vector-dependent factors in both the impurity wave function and phonon energy are not considered in the CC model. However, experimental data shows that only the coupling between the electron and the phonon at the X point is strong.

(3) The A-LO(X) sideband can be easily understood using the indirect transition model. Since the bound energy of the trapped electron in GaP:N is much smaller (~ 10 meV below the conduction band minimum) than energy levels of normal deep trap states (normal deep-trap-state energy levels are larger than 100 meV), its wave function is more localized than normal deep trap wave functions at the X point of the Brillouin zone, even though its wave function is distributed over the entire Brillouin zone. This can be thought of as a "*near-resonant effect*" in the deep trap wave function of GaP:N. This near-resonant effect results in a strong coupling between the phonon and the bound electron at the X point within the indirect transition model. This makes the A-LO(X) band possible.

(4) The A-LO(Γ) band can be partially explained by using the indirect transition model. Since the electron–LO–phonon scattering matrix elements are proportional to $1/K^2$, this implies a strong interaction between the electron and the LO phonon at the Γ point of the Brillouin zone and makes the A-LO(Γ) band possible. More details on all of these points are discussed later in the paper.

This paper is a continuation of previous work in which both the low-temperature luminescence spectrum of the N-bound exciton in GaP (Refs. 4–6) and the associated N-impurity wave function[9] were studied. In particular, by calculating the phonon sideband spectrum using a phonon-assisted, indirect-transition model, it was shown in Ref. 5 that the shape of the phonon sidebands is a sensitive function of the degree of localization of the wave function, and that this model can therefore be used in conjunction with experimental data as a test of the accuracy of impurity wave-function models. In addition to studying the contributions of the above-mentioned near-resonant processes to the phonon sidebands of the GaP:N luminescence, in this paper the indirect-transition model is used to test two impurity wave-function models for nitrogen in GaP by comparing the sideband spectra calculated using these models with the experimental spectrum. The wave-function models which are considered are the Koster-Slater one-band, one-site model[4–6] and the one resulting from the use of our recent semiempirical, multiband formalism.[9] The present calculations also improve upon our previous work[4–6] on phonon sidebands in luminescence by including contributions to these spectra from (1) all three acoustic phonon branches, (2) the optic phonon branches, and (3) the hole transition term in the expression for the sideband spectrum. This is to be contrasted with the calculations presented in Refs. 4–6 which neglected both the optic phonon contribution and the hole-transition term and which included only the longitudinal acoustic and the highest-energy transverse acoustic phonon branches.

We emphasize that direct transitions related to the configuration coordinate model may also contribute to the phonon sidebands in GaP:N. These have been briefly discussed in our previous papers[5,6] and are again briefly discussed below in relation to the longitudinal acoustic and optic phonon sidebands in this system. Furthermore, a simple form of this model is utilized in this paper to demonstrate that some of the low-energy structures observed in the luminescence spectrum can be interpreted as replicas of the spectrum described by our indirect-transition model.

The CC model has been extensively studied, has been applied to numerous systems, and has been widely accepted.[3] On the other hand, while some phonon sidebands in impurity-related luminescence have been recognized as due to indirect transitions through deep-trap states,[10] and while it is known that some experimental data on such sidebands cannot be fully explained using a CC model,[11] the contributions of indirect transitions to impurity-related phonon sideband spectra have not re-

ceived much attention until recently.[4-6] In this paper we demonstrate conclusively that an indirect-transition model, employed along with an accurate deep level wave function,[9] can be used to explain numerous features of the observed GaP:N phonon sideband spectrum.

Finally, we note that other mechanisms, not included in the present model, can also broaden impurity-related phonon sideband features. For example, the effects of alloying[12] and the effects of the Coulomb interaction in donor-acceptor recombination[13] will broaden both the no-phonon line and the related phonon sidebands. In the present paper we limit ourselves to a discussion of spectra due to bound excitons in GaP:N and consider mainly the contributions of our indirect-transition model to the phonon sidebands of this system.

II. FORMALISM

A. The phonon sideband line shape

The bound exciton at the nitrogen site in GaP (with N substituting for P) is comprised of a trapped electron with a wave function which is highly localized in real space and a weakly bound hole.[14] The coupling of the spin $S=\frac{1}{2}$ electron and the $S=\frac{3}{2}$ hole results in two bound exciton states associated with the GaP:N trap. These states are called the A state and the B state and have total angular momentum $J=1$ and 2, respectively. The separation between the A state and the B state is about 1 meV.[1,15] In photoluminescence, the direct transition from the $J=1$ A state to the $J=0$ state produces the A line, while the transition from the $J=2$ B state to the $J=0$ state produces the B line. The higher-energy A line is dipole allowed, while the lower-energy B line is forbidden. Because of the thermal distribution factor, the B line can be observed only at relatively low temperatures.[1,15]

In the case of the indirect, phonon-assisted transitions which are of interest in the present paper, because of the symmetries of the A and B states, these states will in principle couple to phonon modes of different symmetries. One could, in principle, use group theory to determine which phonon modes associated with points, lines, or planes of high symmetry in the Brillouin zone will participate in the indirect, phonon-assisted transitions associated with the A and B states. However, in the case of the N-bound exciton in GaP, the N isoelectronic trap has a wave function which has appreciable amplitude at all K points in the Brillouin zone, even though it is sharply peaked at the X point.[3,9] As is shown in detail below [see Eq. (4)], this factor results in allowed phonon-assisted, indirect transitions for phonons associated with essentially all wave vectors in the Brillouin zone. The forbidden transitions which one would find from a group-theoretical analysis of the A and B states coupling to phonon modes of particular symmetries at isolated points in the Brillouin zone will be far less important than the allowed transition which result from a nonzero wave function at most values of K. In other words, for a deep-trap state such as GaP:N, the selection rules which are dictated by symmetry are relaxed in this sense. An example of this is given in Sec. III.

In what follows, our main interest is in obtaining some physical insight into the origin of the phonon sidebands associated with the A line, and the analogous sidebands associated with the B line are not considered. (The no-phonon lines associated with the A and B states are not considered either.) The primary reason for our studying only the A-line associated phonon sidebands here is that they have been much more extensively studied experimentally than the sidebands belonging to the B line. Furthermore, the B line and its associated sidebands only become important at temperatures much lower[1,15] than the temperature (~ 5 K) at which we choose to compare our theory with experiment. For the temperatures of interest in the present paper, only the A line and its associated sidebands are visible in the experimental spectrum. Thus, only the phonon sidebands associated with the A line are considered below. It is worth pointing out, however, that for reasons discussed in the previous paragraph, our theory makes very little explicit distinction between the A-line and the B-line associated sidebands. In particular, the only place in our formalism where this distinction will occur is in Eq. (4) below, where the no-phonon energy is input into our calculated spectrum. Since we are interested only in the A-line associated phonon sidebands, the experimental A-line no-phonon energy is used in Eq. (4) in the numerical calculations.

A direct transition can occur when the bound electron recombines with the hole at the N site. This transition can be described by first-order time-dependent perturbation theory. In this case, the luminescence intensity corresponding to photon energy $h\nu$ is[3]

$$I_1(h\nu)=\frac{2\pi}{\hbar}\,|\langle\Psi_e|H_{e\text{-ph}}|\Psi_h\rangle|^2\delta(E_e-E_h-h\nu)\,, \quad (1)$$

where $|\Psi_e\rangle$ is the initial-state (electron) wave function, E_e is the bound-electron energy, $|\Psi_h\rangle$ is the final-state (hole) wave function, E_h is the bound-hole energy, and $H_{e\text{-ph}}$ is the electron-photon Hamiltonian for the direct optical transition. The spectrum given by Eq. (1) is often referred to as the no-phonon line and is clearly a zero-width delta function in this approximation. This expression is included here for completeness; the primary focus of this paper is the spectrum of phonon sidebands which accompanies this no-phonon line.

The hole wave function, $|\Psi_h\rangle$, can usually be replaced by the Bloch state at the top of the valence band (at $\mathbf{K}=\mathbf{0}$), $|\phi_{v,0}\rangle$, because it is very localized at the Γ point of the Brillouin zone.[6] On the other hand, the initial state is the deep level state. It can thus be represented as an expansion in terms of Bloch states $|\phi_{n,\mathbf{K}}\rangle$ as

$$|\Psi_e\rangle=\sum_{n,\mathbf{K}}A_n(\mathbf{K})\,|\phi_{n,\mathbf{K}}\rangle\,, \quad (2)$$

where the coefficients $A_n(\mathbf{K})$ can be shown to have the form[3,9]

$$A_n(\mathbf{K})=\frac{\langle\phi_{n,\mathbf{K}}|V|\Psi_e\rangle}{E_e-E_n(\mathbf{K})}\,. \quad (3)$$

Here n is a band index, $\mathbf{K}$ is a wavevector in the first Brillouin zone, $E_n(\mathbf{K})$ is the Bloch-state energy band belonging to $|\phi_{n,\mathbf{K}}\rangle$, and V is the deep-trap potential which produces the bound-electron energy level E_e. In what follows it is assumed that the bound-state energy has the characteristics of a deep level, so that Eq. (2) can be evaluated by using our semiempirical, multiband formalism[9] for deep level wave functions. In the results presented below, the phonon sideband spectrum obtained using this formalism for the wave function is compared both with the experimental spectrum and with the results obtained for the phonon sidebands using the Koster-Slater formalism[4] to evaluate Eq. (2). It is well known that, although the bound-state energy of N in GaP is energetically shallow (~ 10 meV below the GaP conduction band), it possesses many characteristics of a deep level.[2,3] In particular, for this impurity, the wave function is highly localized in real space so that an accurate representation as an expansion in Bloch states, as in Eq. (3), requires many terms in the sum.[3,9]

In order to satisfy momentum conservation ($\Delta\mathbf{K}=\mathbf{0}$), only those coefficients $A_n(\mathbf{K})$ in Eq. (2) with $\mathbf{K}$ values which are equal to or nearly zero will contribute to the line shape for the direct transition, Eq. (1). When a transition involves coefficients $A_n(\mathbf{K})$ which are distributed in other regions of $\mathbf{K}$ space with $\mathbf{K}\neq\mathbf{0}$, first-order perturbation theory fails. That is, a direct transition cannot take place unless $\mathbf{K}$ is zero. Instead, for $\mathbf{K}\neq\mathbf{0}$, indirect transitions with the assistance of phonons are needed to satisfy momentum conservation. Such transitions give rise to phonon sidebands which accompany the no-phonon line. In this case, second-order time-dependent perturbation theory is needed to describe the spectrum, with phonons of the appropriate wave vector to satisfy momentum conservation entering the recombination process.

In previous work it was shown[4-6] that the luminescence spectrum due to the indirect transition (the phonon sideband spectrum) has the form

$$I_2(h\nu)=\frac{2\pi}{\hbar}\sum_{\mathbf{K},\alpha}\delta(h\nu-E_{nP}+h\nu_\alpha(\mathbf{K}))\left|\sum_n A_n(\mathbf{K})\sum_i\left[\frac{\langle\phi_{v,0}|H_p|\phi_{i,0}\rangle\langle\phi_{i,0}|H_\alpha(\mathbf{K})|\phi_{n,\mathbf{K}}\rangle}{E_e-E_i(0)-h\nu_\alpha(\mathbf{K})}+\frac{\langle\phi_{v,0}|H_\alpha(\mathbf{K})|\phi_{i,\mathbf{K}}\rangle\langle\phi_{i,\mathbf{K}}|H_p|\phi_{n,\mathbf{K}}\rangle}{E_h-E_i(\mathbf{K})+h\nu_\alpha(\mathbf{K})}\right]\right|^2, \tag{4}$$

where it has been assumed that the transition is between a trapped electron state and a free or weakly bound hole state, so that the hole wave function can be approximated as a delta function in $\mathbf{K}$ space,[6] and we have expanded the deep-level wave function in Bloch states as in Eq. (2). Here E_{nP}, the no-phonon energy, is the difference between the bound-electron energy and the bound-hole energy E_e-E_h, $h\nu_\alpha(\mathbf{K})$ is the αth branch phonon energy with wave vector $\mathbf{K}$, $|\phi_{i,0}\rangle$ and $|\phi_{i,\mathbf{K}}\rangle$ are intermediate scattering states (at $\mathbf{K}=\mathbf{0}$ and at finite $\mathbf{K}$) associated with the electron transition and the hole transition, respectively, H_α is the electron-phonon Hamiltonian for phonon branch α, H_p is again the electron-photon Hamiltonian (the photon wave vector is assumed negligible), and $E_i(\mathbf{K})$ is the Bloch-state energy band associated with $|\phi_{i,\mathbf{K}}\rangle$. The main contributions to the recombination of the bound exciton in GaP:N come from the Bloch state in the lowest conduction band.[9] As is clear from Eq. (4), the present model includes transitions assisted by phonons which come from essentially all wave vectors in the Brillouin zone and not just from certain critical points such as the X and the Γ points.

There are two steps in the indirect transition. One of these corresponds to changing the electron state by the emission of a photon, and the other one corresponds to changing the electron state by the emission or absorption of a phonon. Since here only the low-temperature transitions are considered, the phonon-absorption effect is not included in Eq. (4). The intermediate states are virtual states, and energy is only conserved in the complete process. However, momentum is, of course, conserved in the process, since otherwise the transition matrix elements vanish. In the calculations presented below, the temperature dependence of the spectrum has been included in the standard way,[16] by multiplying the electron-phonon matrix elements occurring in Eq. (4) by a factor of $1+n(T)$ (for phonon emission), where $n(T)$ is the phonon distribution factor at temperature T.

The two terms in the large parentheses in Eq. (4) represent two different physical processes. In the first process, corresponding to the first term, an electron is first scattered from $\mathbf{K}$ to $\mathbf{K}=\mathbf{0}$ (the Γ point) within the conduction band (which is mainly the lowest conduction band because of the energy denominator and the impurity wave-function structure[9]), with phonon emission, then it makes a vertical transition at the Γ point from the conduction band to the valence band. In the second process, corresponding to the second term in Eq. (4), an electron makes a vertical transition at $\mathbf{K}$ from the conduction band to the valence band, and then a transition within the valence band from $\mathbf{K}$ to the Γ point with phonon emission. These two processes are illustrated schematically in Fig. 1. One can also interpret the latter process as a hole transition from $\mathbf{K}=\mathbf{0}$ in the valence band, via $\mathbf{K}\neq\mathbf{0}$ in the valence band, to $\mathbf{K}$ in the conduction band. Thus, in what follows, the first process is referred to as the electron transition and the second process as the hole transition.

In Eq. (4) only the host lattice phonons are considered. It is well known that impurity-related phonon modes often appear between the acoustic and the optic phonon bands or above the optic phonon bands.[16] These

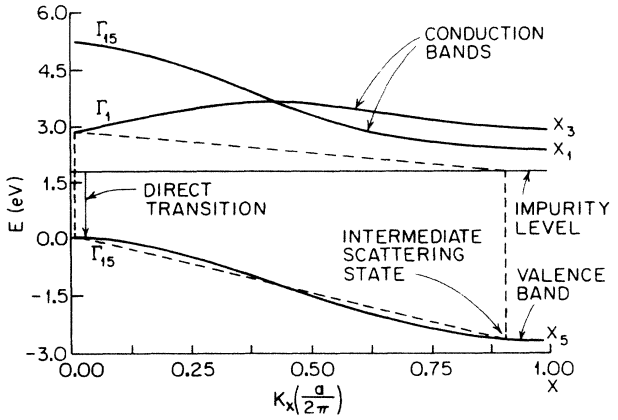

FIG. 1. Electron and hole transitions through an impurity level. Transitions within the lowest two conduction bands and the highest valence band are represented schematically by dashed lines. Indirect transitions through intermediate scattering states in the higher conduction and the lower valence bands are very weak and not shown.

are often referred to as "gap" and "local" phonon modes, respectively, and they are usually distinguishable experimentally from those due to the perfect lattice modes.[17] The energy of the local phonons introduced by N in GaP, which is higher than the energy of the optic phonons, is about 60 meV.[18] Furthermore, the intensity of the associated sidebands, for the small nitrogen concentration considered here, will be much smaller than the intensities of the sidebands associated with bulk phonon modes. In the context of the present theory it is thus practical to ignore the sidebands due to such local modes. Quasilocalized impurity modes also exist in luminescence spectra and are resonant with the lattice phonon bands, typically appearing where the intrinsic phonon state density is low.[19,20] To our knowledge, no quasilocalized modes have been identified in the GaP:N spectra which are considered here, so that such effects are neglected in our calculations.

B. Near-resonant process

From Eq. (4) it can be seen that both near-resonant processes, where the denominator of one or the other of the terms in that equation is close to zero (in practice this will occur only for the second term), and the behavior of the wave-function coefficients $A_n(\mathbf{K})$ as functions of $\mathbf{K}$ are important for determining the shapes and positions of the phonon sidebands. For example, the conduction band of GaP has its minimum at the X point of the Brillouin zone. Furthermore, experimental data show that the bound-electron energy for GaP:N is about 10 meV below the conduction band at that point.[2] Because, by Eq. (3), the $A_n(\mathbf{K})$ are proportional to $1/[E_e - E_n(\mathbf{K})]$, the ratio between the quantity $|A_n(\mathbf{K})|^2$ at the X point and that at the Γ point is about 100 or more. By comparison, the denominator of the electron-transition term does not change significantly as $\mathbf{K}$ changes from the Γ point to the X point of the Brillouin zone. Thus, for this term, the line shape for phonon-assisted indirect recombination of the bound exciton will be strongly affected by the shape of the $A_n(\mathbf{K})$ and only weakly affected by the energy denominator. On the other hand, the denominator of the hole-transition term in Eq. (4) can become very small near the center of the Brillouin zone (the Γ point), while the coefficients $A_n(\mathbf{K})$ have relatively large denominators at that point. Thus, the contribution of this term to the shape of the phonon sideband spectrum is dominated largely by the near-resonant process which cause the energy denominator to become small, and is only weakly affected by the shape of the $A_n(\mathbf{K})$. Therefore, for $\mathbf{K}$ near the X point, the sidebands due to such emission processes are strongly affected by the shape of the $A_n(\mathbf{K})$, while for $\mathbf{K}$ near the Γ point, near-resonant processes dominate their behavior. Of course, the general overall shape of the sidebands must be obtained by superposition of the effects just described with the shape of the phonon state density. Furthermore, since Eq. (4) involves the square of the sum of the hole and electron transition terms, there will also be an interference effect between these two terms.

C. Models for band structure, phonon state density, and matrix elements

Equation (4) clearly links many properties of the defect and the perfect crystal with the phonon sideband spectrum. Among these are the impurity wave-function coefficients $A_n(\mathbf{K})$, as discussed above, the impurity electron and hole bound-state energies E_e and E_h, the host-crystal phonon-dispersion relations and state density, the host-crystal energy band structure, and the phonon scattering matrix elements. As has just been mentioned, the calculated phonon sideband line shapes are sensitive to the choices of the $A_n(\mathbf{K})$ and to the relations between E_e and E_h and the host band structure. It is also clear from the form of Eq. (4) that the general shape of the phonon sidebands, especially in regard to the positions of the major peaks, is strongly dependent on the host phonon state density. For a reasonable choice for this quantity and for a reasonable choice of host band structure, these spectra are very sensitive functions of the coefficients $A_n(\mathbf{K})$. For example, the wave function for GaP:N from the Koster-Slater one-band, one-site model[21,22] is highly localized at the X point in the Brillouin zone. On the other hand, the wave functions obtained from both our semiempirical formalism[9] and Jaros's more sophisticated calculation[3] are more spread out in the Brillouin zone than the Koster-Slater wave function. Thus, these types of wave functions will give significantly different phonon sidebands when used as input into Eq. (4) than those computed using the Koster-Slater model. Such wave-function models can therefore clearly be tested by using the wave functions which result from them in Eq. (4) and comparing the resulting spectra with the experimental phonon sideband spectrum to see which wave function produces a spectrum in closest agreement with the

experimental data.

In the calculations of the phonon sideband spectrum for GaP:N presented below, the phonon-dispersion relations and state density that result from the use of the second-neighbor force-constant model developed by Banerjee and Varshni[23,24] are used. In this model the force-constant parameters were chosen so that the dispersion relations accurately reproduce neutron scattering data for GaP.[23,24] In contrast to our previous work which used this model,[4–6] the optic as well as the acoustic phonon branches have been included in the calculation. Furthermore, the long-ranged Coulomb forces, left out of the previous calculations, have been included in the present paper. The primary effect of these interactions is to cause a splitting of the LO and TO phonon branches at the Γ point.

As is briefly discussed in Refs. 5 and 6, the electron-phonon scattering matrix elements $\langle \phi_{n,0} | H_\alpha(\mathbf{K}) | \phi_{n,\mathbf{K}} \rangle$ which enter the sideband spectrum, Eq. (4), are very complicated. In principle, they can be modeled through the use of a deformation potential approach.[16,25] Instead, for simplicity, in the present paper these matrix elements are described by using analytic forms which should produce the qualitatively correct behavior for these quantities. For both the LA and TA phonon modes it is assumed that these matrix elements have a form that has been shown to be valid for the electron-LA phonon scattering matrix element in metals.[25] This is

$$\langle H_\alpha(\mathbf{K}) \rangle = C_\alpha [\sin(|\mathbf{K}| r_s) - |\mathbf{K}| r_s \cos(|\mathbf{K}| r_s)] / |\mathbf{K}|^2, \quad \alpha = 1,2,3 \tag{5}$$

where $|\mathbf{K}|$ is the magnitude of the phonon wave vector, C_α is the coupling strength for each acoustic phonon branch α, the index α runs over the three acoustic phonon branches with $\alpha=1$ and 2 corresponding, respectively, to the lowest and highest TA branches and $\alpha=3$ corresponding to the LA branch, and r_s is the radius of a sphere close in size to the Wigner-Seitz cell. As is discussed below, in what follows r_s is slightly adjusted to obtain better agreement between the experimental and theoretical phonon sidebands. The expression, Eq. (5), for the LA and TA scattering matrix elements has the property that it is flat at the zone edge and drops smoothly to zero at the zone center. For the longitudinal-optic phonon branches, a form similar to that derived in Ref. 16 for the polaron problem (which involves LO-phonon, electron coupling) is assumed,

$$\langle H_\alpha(\mathbf{K}) \rangle = \begin{cases} C_\alpha / |\mathbf{K}|, & |\mathbf{K}| > K_0 \\ C'_\alpha, & |\mathbf{K}| \le K_0 \end{cases} \tag{6}$$

for $\alpha=6$, where C_α and C'_α have similar meanings here as for the acoustic branches, and K_0 is an adjustable parameter that plays a role similar to that of r_s in Eq. (5). For the transverse optic branches, the electron-phonon matrix element is difficult to model. For simplicity, we assume that it is a constant, that is,

$$\langle H_\alpha(\mathbf{K}) \rangle = C_\alpha, \quad \alpha = 4,5 . \tag{7}$$

While this matrix element should depend on $\mathbf{K}$, its precise form is complicated. Furthermore, the assumption, Eq. (7), is consistent with some of the assumptions made in Ref. 6. In the calculations presented below, all of the parameters C_α in Eqs. (5)–(7) are adjusted to fit the measured relative heights of the acoustic and optic phonon sidebands.

The photon scattering matrix elements are also needed to determine the phonon sideband spectrum. They are proportional to integrals of the form $\int_{\text{cell}} u_v^*(\mathbf{r},\mathbf{K}) \nabla u_c(\mathbf{r},\mathbf{K}) d\mathbf{r}$,[25] where $u_v^*(\mathbf{r},\mathbf{K})$ and $u_c(\mathbf{r},\mathbf{K})$ are the periodic parts of the Bloch functions associated, respectively, with the valence and conduction bands. In Eq. (4), the photon scattering matrix element associated with the electron-transition term is independent of the wave vector $\mathbf{K}$. The one associated with the hole-transition term mainly represents the direct transition of the electron from the conduction band at wave vector $\mathbf{K}$ to the valence band at the same $\mathbf{K}$. It is thus approximately independent of $\mathbf{K}$. The Bloch state at the Γ point of the lowest conduction band is totally s-like, and it gradually mixes with the states of p-like symmetry as $\mathbf{K}$ approaches the zone edge. On the other hand, the Bloch state at the top of the valence band at the Γ point is totally p-like, and it gradually mixes with the s-like symmetry components as the wave vector approaches the zone edge. These facts cause the integral to vary with $\mathbf{K}$, with the largest value occurring at the zone center. However, this variation with $\mathbf{K}$ is not very great, so that it is assumed that this matrix element is independent of $\mathbf{K}$. This assumption is further justified by the fact that the shapes of the absorption spectra of the perfect GaP crystal are dominated by the electron density of states of the material instead of the photon scattering matrix elements.[25]

The dependence of the phonon and the photon scattering matrix elements on the electronic band number n is not considered in the present theory because transitions involving the higher conduction bands and the lower valence bands are very weak,[16] and the major contributions to the impurity wave function come from the lowest conduction band for GaP:N.[9]

The host band structure, $E_n(\mathbf{K})$, that enters the phonon sideband spectrum, Eq. (4), is modeled using the nearest-neighbor, semiempirical sp^3s^* tight-binding model of Vogl *et al.*[26] As is discussed in Ref. 9, this band-structure model is also used as input into our semiempirical impurity wave-function formalism, which is one of the wave-function models we use to calculate the $A_n(\mathbf{K})$ in the computation of the sidebands. This particular band-structure model has been utilized by a number of investigators successfully to characterize the defect-related electronic properties of numerous semiconductors.[27,28] Thus, it is well tested in application to other problems and should be a reasonably accurate representation of the band structures needed for the calculation of the spectrum using Eq. (4). The sum over the Brillouin zone which is necessary to evaluate Eq. (4) is done numerically using a technique for evaluating gen-

eralized densities of states developed originally by Lehmann and Taut[29] and later modified by Hjalmarson.[30] The bound-state energies of the electron and hole are taken to be 10 and 30 meV,[15,18,31–33] respectively.

III. RESULTS AND DISCUSSION

The results of our calculations of the phonon sideband spectrum for bound excitons in GaP:N, obtained using Eq. (4), are illustrated in Figs. 2(a) and 2(b) for two different impurity wave-function models. In both of these calculated spectra, the temperature was taken to be $T=5$ K. The no-phonon line is not shown in these figures; it would occur at the extreme right-hand edge of the spectrum. In our approximation it is a delta function given by Eq. (1). Figure 2(a) shows the results obtained using the Koster-Slater, one-band, one-site model,[21,22] as in Ref. 5, to evaluate the $A_n(\mathbf{K})$ which enter the sideband spectrum. By contrast, in Fig. 2(b), the phonon sidebands which result from using our recent semiempirical, multiband wave function was shown in Ref. 9 to accurately mimic the wave function obtained from Jaros's[3] more sophisticated calculation; the spectrum in Fig. 2(b) can also be approximately viewed as the phonon sidebands produced by using the latter wave function.

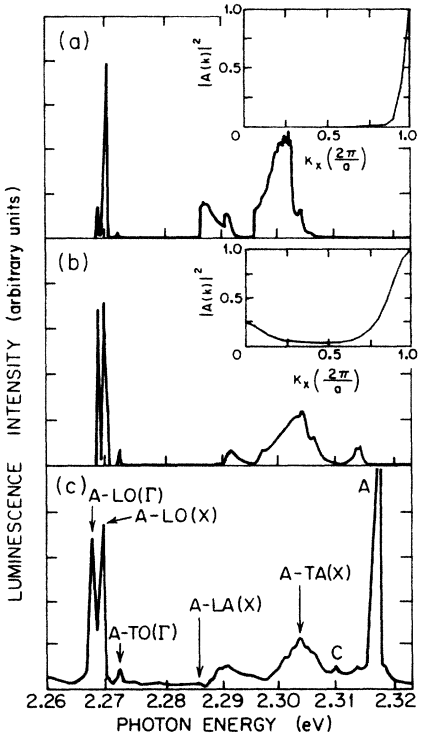

FIG. 2. (a) Calculated phonon sidebands for the nitrogen-bound exciton recombination, using the Koster-Slater one-band, one-site impurity wave-function model (Ref. 21). (b) Calculated phonon sidebands for the nitrogen-bound exciton recombination, using the wave function from our semiempirical, multiband formalism (Ref. 9). (c) Typical photoluminescence spectrum of excitons bound to isolated nitrogen in GaP at $T=5$ K. The excitation was produced by the 4954-Å line of a xenon-ion laser. The energy range is scanned from 2.26 to 2.32 eV (Ref. 34). Insets in (a) and (b) show electron charge densities along K_x for the appropriate wave-function models. The normalization for these charge densities has been chosen so that the contribution from the X point of the Brillouin zone is set equal to 1.

For comparison, in Fig. 2(c), a previously published low-temperature (about 5 K) luminescence spectrum[34] obtained by energetic excitation of a typical sample of GaP containing nitrogen impurities is shown. In this experimental spectrum, the A-exciton line and its various phonon sidebands are labeled using standard notation, where peaks which are thought to be associated with particular types of phonons near particular points in the Brillouin zone are indicated with the prefix A followed by the phonon type and the Brillouin zone point in parenthesis. The well-known B-exciton line and its phonon replica B-LO(Γ) (Ref. 15) do not appear in the experimental spectrum, because of the relatively high temperature of the experiment in Refs. 1 and 34. These features of the spectrum are not relevant to the phonon sidebands considered here. Also, the so-called V band[35] appears as a small shoulder just to the left of the no-phonon A line. At lower temperatures this band becomes more prominent in the spectrum.[35] Finally, the peak labeled C is probably due to some other impurity. In the past it has been identified as belonging to the sulfur donor.[2]

A. General behavior of the spectrum; correlation with wave-function coefficients $A_n(\mathbf{K})$

Although the bound-state energy level of GaP:N is energetically very shallow (about 10 meV below the conduction band), its wave function is highly localized in real space so that deep-level theory gives an adequate description of this isoelectronic trap. The following discussion is valid for both of the wave-function models which have been used to calculate the $A_n(\mathbf{K})$.

Because the bound-state energy E_e is just below the bottom of the conduction band, which occurs very close to the X point in GaP, the wave-function coefficients $A_n(\mathbf{K})$ in Eq. (3), with n corresponding to the lowest conduction band, will be large at that point in the Brillouin zone. This can be thought of as a "near-resonant effect" in the wave function. Furthermore, the bottom of the conduction band is nearly flat over a large region of $\mathbf{K}$ space near the X point, so that many states in the conduction band have similar small denominators and therefore give rise to large wave-function coefficients $A_n(\mathbf{K})$ for the lowest conduction band. On the other hand, near the Γ point the $A_n(\mathbf{K})$ for the lowest conduction band are relatively small due to the fact that the energy denominator in Eq. (3) is large. However, at least in the wave-function formalism of Ref. 9, the $A_n(\mathbf{K})$ are still larger at this point than one would expect for the corresponding wave-function coefficients of a shallow donor.[7]

We remark in passing that these features of the wave function may provide clues to the reason for the high quantum efficiency of GaP:N. The deeply bound elec-

tron wave function is s-like and the weakly bound hole wave function is p-like,[36] so that the direct transition is allowed by the dipole-selection rule. The intensity of the no-phonon line is closely related to the magnitude of the deep-level wave function at the Γ point by Eq. (1); the larger the wave function at $\mathbf{K}=\mathbf{0}$, the stronger the no-phonon line. This fact has also been pointed out by others.[2]

The shape and relative strengths and widths of several of the peaks in the phonon sideband spectra of Figs. 2(a)–2(c) can be qualitatively understood using these considerations. On the basis of these arguments, one would expect that the peaks coming mainly from phonons near the X point will be enhanced. It is clear in both the experimental and the theoretical spectra [especially that which results from using the multiband approximation to $A_n(\mathbf{K})$ in Fig. 2(b)] that this expectation is realized. In particular, the A-TA(X) and A-LA(X) bands are strong and broad. Similarly, this is the reason that the A-LO(X) band is slightly broader than the A-LO(Γ) and A-TO(Γ) bands. On the other hand, the reason that the bands associated with the optic phonons are much narrower than those associated with acoustic phonons is traceable to the small dispersion of the optic phonons in comparison with the acoustic branches, which gives rise to narrower peaks in the density of states.[23,24]

We have mentioned in Sec. II that symmetry-imposed selection rules are relaxed for phonon-assisted, indirect transitions related to the GaP:N deep trap. This can be seen clearly if we compare the optical sidebands in the spectra of pure GaP, GaP:S, and GaP:N. Pure GaP has translationally invariant perfect lattice. Thus an electron in the conduction band at the $X_{1,C}$ point is perfectly described by a Bloch state at $X_{1,C}$. Thus, by symmetry-imposed selection rules, optic phonons at the X point will not scatter the electron at $X_{1,C}$ to the conduction band $\Gamma_{1,C}$. Instead, it will scatter the electron from $X_{1,C}$ to the conduction band at $\Gamma_{15,C}$. This scattering is difficult to detect in optical spectra because of its large energy denominator.[37,38] In the GaP:S shallow trap state, the trapped electron wave function is highly localized in the X point but also has small components near that point. While its primary amplitude is well represented by a Bloch state at $X_{1,C}$, there are also small components for the values of K near, but not at, the X point. Because of these small but nonzero components of the wave function near the X point, phonons with corresponding wave vectors can assist the electronic transition from $X_{1,C}$ to the $\Gamma_{1,C}$ point and this transition becomes allowed. In fact, this is why there is a small LO(X) phonon sideband in the luminescence spectrum of GaP:S.[7] Since the wave-function amplitude at the points near the X point is small, however, the intensity of the LO(X) band is weaker than that of the LO(Γ) band. Finally, the wave function of the GaP:N deep trap is more delocalized[3,9] in the Brillouin zone than that of GaP:S. In particular, the components of the nitrogen wave function which have values which are close to but not equal to the X point are much larger than the corresponding components for GaP:S. Thus, the LO(X) phonon sideband in GaP:N is very strong.[39] This implies that symmetry-induced forbidden phonon scattering between two isolated points in the Brillouin zone is not necessarily important for understanding phonon-assisted transitions through a deep-trap state.

B. A near-resonant process

In the experimental spectrum of Fig. 2(c) there is a very broad, nonzero signal background between the no-phonon line and the A-TA(X) sideband. This kind of signal is a common feature for excitons bound to neutral impurities.[7] In addition, there is a band near 2.314 eV, which occurs only as a small shoulder in Fig. 2(c), but which has been observed and studied in more detail by others.[35,40–43] The latter band has been denoted as the V band in the literature.[35,43] We now briefly discuss these features within the context of the present indirect-transition model.

The broad background feature cannot occur in our calculation if only the electron-transition term in Eq. (4) is included. However, it can be simulated by including both the hole transition and the electron-transition terms. For i referred to the highest valence band and for $\mathbf{K}$ near the Γ point, the contribution to the denominator of the second term in Eq. (4) (the hole-transition term) is very small for the acoustic phonon branches. This causes an enhancement of this term under these conditions. That is, there is a near-resonance in this case. Furthermore, if this near-resonant phenomenon is strong enough, it can compensate for the low acoustic phonon state density in this region of $\mathbf{K}$ space. In other words, when the hole-transition term is near resonance, one expects a moderate signal background in the phonon sideband spectrum even though the phonon density of states is small there. This is confirmed by our calculations, as illustrated in Fig. 2(b), where we find a nonzero signal background between the A-TA(X) band and the no-phonon line, which has its origin in this effect. If the hole-transition term is neglected, as in the calculation illustrated in Fig. 2(a), the structure disappears completely. A similar effect might explain the nonzero signal background in the spectra of excitons bound to neutral donors such as sulfur, selenium, and tellurium in GaP.[7] In our calculations of the hole-transition term, we have neglected the optic phonons because of their relatively large energy denominators. The relative strengths of the acoustic phonon matrix elements used for evaluating the hole-transition term have been taken to be the same as the ones used for the electron transition term.

As can be seen in Fig. 2(b), our calculations of the sideband spectrum including the hole-transition term also produce a band centered near 2.314 eV in the spectrum, which correlates well with the position of the V band.[35] However, the agreement with experiment in this case may be fortuitous, since the sp^3s^* band-structure model[26] produces a valence-band effective mass at the Γ point which is in disagreement with experiment,[44] and as is discussed above, the enhancement of the hole-transition term depends crucially on the small-$\mathbf{K}$ behavior of the valence band. Furthermore, the resonant be-

havior of this term also clearly depends strongly on the behavior of the acoustic phonon dispersion relations at small **K**. Thus, the fact that the present indirect-transition model predicts a peak at almost precisely the experimental value of the V band might be more an artifact of our choice of electronic band and phonon force-constant parameters than an explanation for the physical origin of the V band itself. However, we believe that for any reasonable choice of parameters, the hole-transition term will produce a peak in the spectrum at *some* energy between the A line and the A-TA(X) sideband. In view of recent and past experimental studies.[35,40] however, present model clearly cannot explain all of the properties of this interesting spectral feature, such as its temperature-dependent features, and its properties observed in below the band-gap resonant excitation experiments[40] and time-resolved measurements.[40]

The V band, as well as the undulation structure which has been observed to be superimposed upon it, has been well studied experimentally.[35,40–42] In particular, it has been observed that the separation between this band and the B line is about equal to the separation between the A line and the B line and that, furthermore, the V band becomes stronger under conditions where the B-exciton line is enhanced. Some authors have thus interpreted this band as an acoustic phonon sideband of the B line.[43] In addition, Street and Wiesner[40] have shown that the undulation structure consists of a series of no-phonon lines of excitons bound to nitrogen-acceptor pairs. Recent experiments[35] have confirmed that the V band and the undulation structure arise from two distinct types of effects. Furthermore, the experimental results[35,40,43] seem to suggest that the V band might be due to more than one perturbation source. We suggest on the basis of the present calculations that the indirect transition mechanism might be one of the possible sources of this band, since we expect that both the broad background and the peak coming from the hole-transition term will occur for any reasonable choice of parameters used with our formalism. While, as is mentioned above, the exact *position* of the peak is sensitive to the choice of parameters, the *existence* of the peak should be independent of the choice.

C. Variation of phonon sidebands with impurity wave-function model; comparison with experiment

A comparison of the two theoretical phonon sideband spectra, Figs. 2(a) and 2(b), with the experimental spectrum, Fig. 2(c), shows clearly that the spectrum obtained using our semiempirical multiband formalism [Fig. 2(b)] for the bound-electron wave function in GaP:N reproduces the data much more accurately than that which is obtained using the Koster-Slater one-band, one-site approximation for this wave function. One of the main reasons for the differences in the spectra produced by the two wave-function models is that the Koster-Slater wave function is highly localized at the X point of the Brillouin zone, whereas the wave function resulting from our formalism is more spread out in **K** space[9] than the Koster-Slater wave function. In particular, the wave function coming from the formalism of Ref. 9 has a squared amplitude at the Γ point which is about 10% of its value at the X point. By contrast, the Koster-Slater wave-function model produces a ratio between the squared amplitudes at the Γ and X points of about 0.03%.

This fact can qualitatively explain several features in the phonon sideband spectra. Conversely, an analysis of the spectra can be used to infer that the impurity wave function cannot be as highly localized at the X point as the Koster-Slater wave-function model predicts. For example, from Fig. 2(a), it can be seen that the Koster-Slater wave function introduces an extra peak in the LA phonon sideband which is not present in the experimental spectrum, Fig. 2(c). This can be understood by the following analysis. The phonon-dispersion relations and the resulting state density[23,24,45] show that the energies of the LA phonons at the X point of the Brillouin zone are about 31 meV and that the peak of LA phonon state density occurs at about 26 meV. If the impurity wave function was as highly localized at the X point as the Koster-Slater model predicts, it would mainly couple with the phonons at the zone edge and thus compensate the low state density of the LA phonons at that point. There would then be a peak appearing at about 2.286 eV in the spectrum, as is indicated by the arrow in Fig. 2(c), which is labeled A-LA(X) (at about 31 meV below the no-phonon line). This is indeed confirmed by the extra LA peak in Fig. 2(a). Furthermore, the luminescence spectra of shallow donor impurities in GaP, such as sulfur,[7] show a peak at about this position below the no-phonon line, indicating a highly localized wave function at the X point. However, both the nitrogen experimental data, Fig. 2(c), and the theoretical spectrum obtained using the semiempirical formalism for the nitrogen wave function, Fig. 2(b), show that the LA phonon sideband is located at about 2.291 eV, i.e., about 26 meV below the no-phonon line. This means that the LA phonons involved in the indirect transition are mainly associated with energies less than 31 meV and that the impurity wave function is not as highly localized at the X point of the Brillouin zone as the Koster-Slater model predicts. We emphasize again that our indirect-transition model includes transitions assisted by phonons at essentially all points of the Brillouin zone. This aspect of our model, coupled with our use of a reasonably accurate deep-level wave function, enables us to reproduce the LA phonon peak at about the correct position [to the right of the LA(X) position in Fig. 2(c)].

The transverse acoustic phonon sidebands can be understood mostly on the basis of the phonon-dispersion relations and state density.[23,24] Although an effect similar to that which occurs with the LA phonons also occurs in this case, the resulting shift in the TA phonon peak is much smaller than the corresponding LA peak shift. The dispersion relation for the TA phonons has two branches. The phonons associated with the lower branch are related to the peaks which occur in Fig. 2(b) as a shoulder of the A-TA band at about 2.305 eV. The phonons associated with the higher branch are related to the main A-TA band in Figs. 2. If the lower transverse

acoustic phonon branch is neglected, as in the calculation in Ref. 5 and Fig. 2(a), the shoulder of the A-TA band disappears completely.[5] In order to best fit the experimental data, we have taken the ratio of the relative strengths of the electron-acoustic phonon matrix elements as $C_1/C_2=0.3$ and $C_1/C_3=0.8$.

The relative distances from the no-phonon line to the A-TA and A-LA bands are worth discussing. In particular, the distance to the center of the A-LA peak is about twice that to the center of A-TA band. This might lead one to believe that the A-LA band is a phonon replica of the A-TA band, caused by a CC interaction instead of by the indirect-transition mechanism used here. However, it should be noted that the position of the peak in the LA band in the experimental spectrum [Fig. 2(c)] is consistent with that of the LA peak in the phonon state density.[23–45] This leads in the present model to a peak at that position in the theoretical sideband spectrum [Figs. 2(a) and 2(b)]. Also, a comparison of the general shapes of the experimental and theoretical A-LA peaks lends support to our conjecture that the A-LA band is primarily due to the indirect-transition mechanism. However, our model produces a peak which is slightly sharper than the experimental peak [Fig. 2(b)]. It is thus possible that the A-LA band is produced by some combination of indirect and CC transitions, because the latter type of transition could produce a broader peak than that which occurs in the experimental spectrum.[44] We note that phonon replicas found in the optical spectra of other defect-host systems have been shown to be well reproduced by a model which includes CC coupling due to acoustic phonons.[46]

In all calculations of the acoustic phonon matrix elements, Eq. (5) has been evaluated in the following manner. A spherical shell of radius r_s surrounding the primitive cell was considered and r_s was treated as an adjustable parameter. It was found that the line shape of the LA phonon sideband is not sensitive to a small change in r_s, but that the line shape of the TA sideband is somewhat sensitive to this parameter. Further, it was found that the value of r_s which best fits the acoustic phonon sideband data is about 10% larger than the radius of the Wigner-Seitz cell.

It has been suggested[47] that the A-LO(Γ) band is due to a CC interaction. This is supported by the quantitative results of using the indirect-transition theory to fit the experimental LO phonon sideband spectrum. In the spectra shown in Figs. 2(a) and 2(b), we have chosen $C_1/C_6=0.06$, $C_1/C_6'=0.08$, and K_0 equal to $0.15(2\pi/a)$, where a is the lattice constant. Although the fit is reasonably good, the coefficients C_6 and C_6' are required to be about an order of magnitude larger than those for the other phonon branches. The analysis in Sec. III D also indicates that the indirect-transition contribution to the LO phonon sideband is an order of magnitude weaker than the contribution from the CC interaction.

Experiments have indicated that the A-TO band is due to the phonons of the TO branches near the Γ point.[2] However, in our calculation this band comes from the phonons near the X point. We speculate that this difference is traceable to a polariton effect.[16] It is well known that the coupling between TO phonons and photons is often strong enought to produce polaritons. This interaction causes changes in the TO phonon-dispersion relation, making the phonon energy lower at the Γ point than at the X point. The TO dispersion relation of Banerjee and Varshni,[23,24] used in the present model, has just the reverse behavior. This fact makes use of a better approximation for the TO electron-phonon matrix elements, Eq. (7), somewhat pointless within the present approach. That is, in our calculation, we have not included the effect of polaritons, so that the positions of the A-TO bands are not predicted accurately. Finally, in our calculations, we have used $C_1/C_4=0.5$ and $C_1/C_5=0.8$ for the TO phonon matrix elements.

D. Phonon replicas of the indirect-transition spectrum

If the experimental spectrum of Fig. 2(c) is continued in energy below the optic bands (below about 2.27 eV), considerable structure, occurring at energies between about 2.22 and 2.27 eV is observed.[48] This extended experimental spectrum is shown in Fig. 3(a). In that figure, it can be seen that the bands in this lower-energy region are similar in appearance to, but weaker in intensity that, those described by the indirect-transition spectrum just discussed. Furthermore, each feature of this

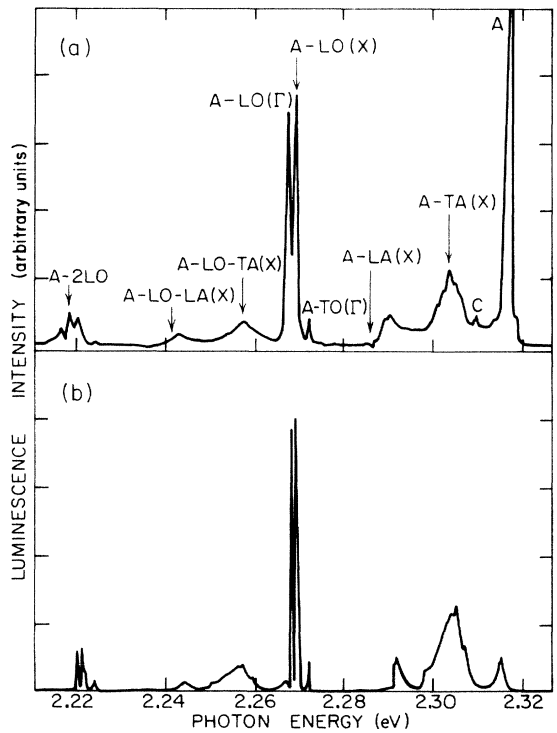

FIG. 3. (a) Typical photoluminescence spectrum of excitons bound to isolated nitrogen in GaP at $T=5$ K. The excitation was produced by the 4954-Å line of a xenon-ion laser. The energy range is scanned from 2.22 to 2.32 eV (Ref. 48). (b) Simulation of the experimental data of (a) by Eq. (8). Here $S=0.3$ and only the terms $m=0$ and $m=1$ have been kept.

part of the spectrum is shifted down in energy from a corresponding, similarly shaped, feature in the higher-energy spectrum by almost exactly one longitudinal optic phonon energy (about 50 meV). One possibility for the origin of these bands is that they might be due to a third-order indirect transition involving two optic phonons and one acoustic phonon. However, if this were the case, one would expect the bands at 2.24 and 2.255 eV to contain some sharply peaked features because of the overlap integral between the optic and acoustic phonon state densities which would result from such a third-order transition. As can be clearly seen in Fig. 3(a), however, these two peaks are very smooth in shape, with no sharp features present. From Fig. 3(a), it can also be seen that the sharp peaks at 2.22 eV are almost exactly two longitudinal optic phonon energies below the no-phonon line.

These facts lend support to the hypothesis that these weak sidebands are replicas of the indirect-transition spectrum which are caused by CC mode coupling with the longitudinal optic phonons. If this is the case, then the A-LO peaks in Figs. 2 must contain contributions from both indirect transition and CC coupling. In order to determine the relative contributions of these two processes to these peaks and to try to reproduce the weak low-energy sidebands, we have modified the theory described above to account for such a coupling[3] and have calculated the resulting spectrum including this modification. If CC mode coupling is allowed only with the longitudinal optic phonons, it is not difficult to show that the resulting spectrum has the form

$$I(h\nu)=\sum_{m=0}^{\infty} I_2(h\nu-mh\nu_0)e^{-S}S^m/m!\,, \tag{8}$$

where $I_2(h\nu)$ is the indirect-transition spectrum, given by Eq. (4), $h\nu_0$ is the LO phonon energy, $h\nu_0=50$ meV,[24,45] S is the Huang-Rhys dimensionless coupling parameter,[3] and m is the quantum number of the CC vibrational states.

The A-TA peak at 2.305 eV contains no contributions from CC interactions with the LO phonons. It is furthermore reasonable to assume that the smaller peak at 2.255 eV, labeled A-LO-TA, is a replica of the A-TA peak, induced by a CC interaction with the LO phonons. In order to make this assumption quantitative, we have used Eq. (8), keeping only the $m=0$ and 1 terms, limiting I_2 to contain only the transverse acoustic sideband of the indirect-transition spectrum, and treating S as a variable parameter. We have then adjusted S, so that the relative heights of the A-TA-LO and A-TA peaks which are shown in Fig. 3(a) are reproduced by Eq. (8) under these conditions. This procedure gives the approximate Huang-Rhys factor of $S=0.3$, corresponding to the relative strength of the LO phonon coupling to the TA part of the indirect-transition spectrum. By way of comparison, the value of $S=0.35$ found by others[8] using a CC model for the LO phonons in GaP:N is slightly larger than our value.

Using Eq. (8) it can be shown that the proportion of the A-LO peak intensities contributed by indirect transitions, relative to the total A-LO peak intensity, is given by

$$\frac{I_i}{I_t}=\left[\frac{2}{S}\frac{I'}{I_t}-1\right], \tag{9}$$

where I_t is the total (experimental) intensity of the A-LO peak, I_i is the intensity of this peak predicted by the indirect transition model [i.e., it is the LO portion of the phonon sideband spectrum $I_2(h\nu)$ predicted by Eq. (4)], and I' is the intensity of the peak labeled A-2LO in Fig. 3(a). Using the value of $S=0.3$ from the above discussion and obtaining $I'/I_t=0.16$ from Fig. 3(a), we find that the relative strength of the indirect-transition contributions to the A-LO peak, I'/I_t, is on the order 10%. This simple calculation and the discussion in Sec. III C lends support to the idea that despite the ability of the indirect transition model to fit the measured longitudinal optic phonon sidebands, they are caused primarily by CC interactions.

In order to further test the reasonable hypothesis that the weak, low-energy sidebands in Fig. 3(a) are, at least partially, CC phonon replicas of the indirect-transition spectrum, we have calculated the spectrum resulting from Eq. (8) when the entire indirect-transition spectrum $I_2(h\nu)$, Eq. (4), is inserted into it and when only the first two terms ($m=0$ and 1) are kept. In this calculation, we have used the above determined value for the Huang-Rhys factor of $S=0.3$. The use of this value of S for the entire spectrum is justified by noting that, within the harmonic approximation (no coupling between phonon modes), the strength of the CC interaction with the LO phonons is the same for both the direct and the indirect transitions.[6] Thus, the value of S found by fitting only the A-TA and A-LO-TA peak intensities, as was done above, should be applicable to the entire spectrum between, and including, the no-phonon A line and the A-LO phonon sideband.

In Fig. 3(b) we show the spectrum that results from this calculation. As can be seen in comparison of Figs. 3(a) and 3(b), the theoretical fit to the experimental spectrum is quite reasonable, indicating that the low-energy sidebands can be at least partially explained as replicas of the indirect-transition spectrum.

IV. SUMMARY AND CONCLUSIONS

In summary, the indirect transition model should be used for GaP:N because (a) the indirect-transition spectra may not be neglected in some cases even when the dipole-allowed direct transition appears, (b) the near-resonant effect of the deep-trap wave function plays an important role in recombination, (c) the Huang-Rhys factor is small for GaP:N, and (d) it is especially necessary to use the second-order transition theory to understand in detail the features of the sideband spectrum of GaP:N.

Many features of the sideband structures can be understood within the context of this model by detailed consideration of a combination of the following three factors: (1) the behavior of the impurity wave function in **K** space (a near-resonant effect in the wave function),

(2) a near-resonant process which enters the energy denominator in the expression for the sideband spectrum, and (3) the shapes of the phonon-dispersion relations and state density. Using this model, we have tested two impurity wave-function models, the Koster-Slater one-band, one-site model and the one resulting from our recent semiempirical multiband model.[9] The latter wave function, which is relatively delocalized in **K** space, yields a sideband spectrum which is in better agreement with the experimental spectrum than that coming from the Koster-Slater model, which is highly localized at the X point. Thus, we conclude that the wave function of N in GaP is delocalized in **K** space, as is characteristic of deep-level wave functions in general. We have also studied the effect on the sideband spectrum of modifying the LA phonon scattering matrix element and comparing with the experimental data. This shows that a slightly modified matrix element needs to be used to accurately calculate the LA and TA sidebands. Perhaps further work should investigate the possibility of utilizing more accurate forms for the phonon scattering matrix elements and of attempting to study these quantities in detail. In addition, our studies suggest that a near-resonant process might be one of the possible sources for the V band. Given recent experimental developments regarding this interesting spectral feature,[35] however, it is clear that the mechanism considered here cannot account for all of the features of the V band. Furthermore, the fact that the present calculations have yielded a peak at exactly the experimental V-band energy is probably a fortuitous result of our choice of parameters to characterize the electron bands and the phonon dispersion relations. In addition, we have also explained why the position of the A-LA band in the GaP:N spectrum is different from the one due to a normal shallow trap. In this work we have also included for the first time both the optic and lower-energy transverse acoustic phonons as well as the hole-transition term in our calculations of the phonon sidebands within the indirect transition model. Finally, we have shown that the sidebands which occur in the data below 2.27 eV in energy can be, at least partially, explained using combined CC and indirect-transition models, as phonon replicas of the indirect-transition spectrum.

ACKNOWLEDGMENTS

We gratefully acknowledge the support of National Science Foundation Grant No. ECS-84-07185, the Air Force Office of Scientific Research, and the Army Research Office. We thank H. P. Hjalmarson for his interest in this problem, for his careful criticisms of several versions of the manuscript, for pointing out several references, and for many stimulating conversations.

[1]D. G. Thomas, M. Gershenzon, and J. J. Hopfield, Phys. Rev. **131**, 2397 (1963).
[2]P. J. Dean, J. Lumin. **1/2**, 398 (1970).
[3]M. Jaros, *Deep Levels in Semiconductors* (Adam Hilger, Bristol, 1982).
[4]P. G. Snyder, M. A. Gundersen, and C. W. Myles, J. Lumin. **31/32**, 448 (1984).
[5]P. G. Snyder, C. W. Myles, M. A. Gundersen, and H. H. Dai, Phys. Rev. B **32**, 2685 (1985).
[6]P. G. Snyder, PhD thesis, University of Southern California, 1984 (unpublished).
[7]P. J. Dean, Phys. Rev. **157**, 655 (1967).
[8]D. J. Wolford, W. Y. Hsu, J. D. Dow, and B. G. Streetman, J. Lumin. **18/19**, 863 (1979).
[9]H. H. Dai, M. A. Gundersen, and C. W. Myles, Phys. Rev. B **33**, 8234 (1986).
[10]A. T. Vink, R. L. A. van der Heijden, and A. C. van Amstel, J. Lumin. **9**, 180 (1974).
[11]H. Chang, C. Hirlimann, M. Kanehisa, and M. Balkanski, Sci. Sin. **25**, 942 (1982).
[12]D. J. Wolford, B. G. Streetman, and J. Thompson, J. Phys. Soc. Jpn. **49**, 223 (1980).
[13]D. G. Thomas, J. J. Hopfield, and W. M. Augustyniak, Phys. Rev. **140**, A202 (1965).
[14]J. J. Hopfield, D. G. Thomas, and R. T. Lynch, Phys. Rev. Lett. **17**, 312 (1966).
[15]J. J. Hopfield, P. J. Dean, and D. G. Thomas, Phys. Rev. **158**, 748 (1967).
[16]O. Madelung, *Introduction to Solid-State Theory* (Springer-Verlag, Berlin, 1978).
[17]O. Madelung, *Advances in Solid State Physics* (Pergamon Vieweg, Munster, 1971).
[18]D. G. Thomas and J. J. Hopfield, Phys. Rev. **150**, 680 (1966).
[19]T. N. Morgan, B. Welber, and R. N. Bhargava, Phys. Rev. **166**, 751 (1968).
[20]C. H. Henry, P. J. Dean, and J. D. Cuthbert, Phys. Rev. **166**, 754 (1968).
[21]G. F. Koster and J. C. Slater, Phys. Rev. **95**, 1167 (1954).
[22]R. A. Faulkner, Phys. Rev. **125**, 991 (1968).
[23]R. Banerjee and Y. P. Varshni, Can. J. Phys. **47**, 451 (1969).
[24]R. Banerjee and Y. P. Varshni, J. Phys. Soc. Jpn. **30**, 1015 (1971).
[25]H. Bube, *Electronic Properties of Crystalline Solids* (Academic, New York, 1974).
[26]P. Vogl, H. P. Hjalmarson, and J. D. Dow, J. Phys. Chem. Solids **44**, 365 (1983).
[27]H. P. Hjalmarson, P. Vogl, D. J. Wolford, and J. D. Dow, Phys. Rev. Lett. **44**, 810 (1980).
[28]See, for example, C. W. Myles, P. F. Williams, E. G. Bylander, and R. A. Chapman, J. Appl. Phys. **57**, 5279 (1985); C. W. Myles and O. F. Sankey, Phys. Rev. B **29**, 6810 (1984); O. F. Sankey and J. D. Dow, Appl. Phys. Lett. **38**, 685 (1981); J. Appl. Phys. **52**, 5139 (1981); J. D. Dow, R. E. Allen, O. F. Sankey, J. P. Buisson, and H. P. Hjalmarson, J. Vac. Sci. Technol. **19**, 502 (1981).
[29]M. Lehmann and R. Taut, Physica Status Solidi B **54**, 469 (1972).
[30]H. P. Hjalmarson, PhD thesis, University of Illinois at Urbana-Champaign, 1979 (unpublished).
[31]W. Y. Hsu, J. D. Dow, D. J. Wolford, and B. G. Streetman, Phys. Rev. B **16**, 1597 (1977).
[32]E. Cohen and M. D. Sturge, Phys. Rev. B **16**, 1039 (1977).
[33]E. Cohen, M. D. Sturge, N. O. Lipari, M. Altarelli, and A. Baldereschi, Phys. Rev. Lett. **35**, 1591 (1975).

[34]M. A. Gundersen and W. L. Faust, J. Appl. Phys. **44**, 376 (1973).
[35]D. Gershoni and E. Cohen, J. Lumin. **34**, 83 (1985).
[36]T. N. Morgan, Phys. Rev. Lett. **21**, 819 (1968).
[37]Orest J. Glembocki and Fred H. Pollak, Phys. Rev. B **25**, 1179 (1982).
[38]Orest J. Glembocki and Fred H. Pollak, Phys. Rev. B **25**, 1193 (1982).
[39]Strictly speaking the optic phonons which contribute to the LO(X) band are not precisely from the X point of the Brillouin zone. Instead, they come from points very close to the X point. We neglect such small differences and, by convention, still call this phonon sideband the LO(X) band.
[40]R. A. Street and P. J. Wiesner, Phys. Rev. B **14**, 632 (1976).
[41]J. J. Hopfield, H. Kukimoto, and P. J. Dean, Phys. Rev. Lett. **27**, 139 (1971).
[42]T. N. Morgan, M. R. Lorenz, and A. Onton, Phys. Rev. Lett. **28**, 906 (1972).
[43]J. L. Merz, R. A. Faulkner, and P. J. Dean, Phys. Rev. **188**, 1229 (1969).
[44]H. P. Hjalmarson (private communication).
[45]H. Bilz and W. Kress, *Phonon Dispersion Relations in Insulators* (Springer-Verlag, Berlin, 1979).
[46]H. P. Hjalmarson, L. A. Romero, D. C. Ghiglia, E. D. Jones, and C. B. Norris, Phys. Rev. B **32**, 4300 (1985).
[47]M. D. Sturge, E. Cohen, and K. F. Rodgers, Phys. Rev. B **15**, 3169 (1977).
[48]M. A. Gundersen (unpublished).